Philosophical Magazine Letters,
Vol. 86, No. 1, January 2006, 47–60

Taylor & Francis
Taylor & Francis Group

In situ straining investigation of slip transfer across α_2 lamellae at room temperature in a lamellar TiAl alloy

J. B. SINGH†, G. MOLÉNAT*‡, M. SUNDARARAMAN†, S. BANERJEE†, G. SAADA§, P. VEYSSIÈRE§ and A. COURET‡

†Materials Science Division, Bhabha Atomic Research Centre, Mumbai, India
‡CEMES, CNRS, BP 94347, 31 055 Toulouse Cedex 4, France
§LEM, CNRS–ONERA, BP 72, 92322 Châtillon, France

(*Received 4 May 2005; in final form 23 November 2005*)

Processes by which deformation spreads throughout a lamellar TiAl alloy have been investigated by *in situ* tensile experiments performed at room temperature in a transmission electron microscope. Several situations are found and analysed in which dislocations cross the γ/α_2 interfaces and the α_2 lamellae – the hard phase of the structure. Conditions by which strain transfer can be elastically mediated across sufficiently thin α_2 lamellae are discussed.

1. Introduction

The microstructure of a two-phase fully lamellar TiAl-based alloy consists of stacks of lamellae of γ TiAl ($L1_0$ structure; figure 1a) and α_2 Ti_3Al (hexagonal $D0_{19}$ structure; figure 1b) with irregular thicknesses and uneven sequences, in such a way that the γ/α_2 interfaces lie along the close-packed planes satisfying the following orientation relationships:

$$(111)_\gamma//(0001)_{\alpha 2} \quad \text{and} \quad \langle 1\bar{1}0]_\gamma//\langle 11\bar{2}0\rangle_{\alpha_2}\dagger$$

This orientation relationship results in a mismatch between lattice positions along the close-packed directions of the two phases (figure 1c).

The γ phase is softer than α_2 and difficulties arising in transferring deformation from γ to α_2 through these interfaces are regarded as a cause of sample fracture [2]. In view of the large number of such γ/α_2 interfaces, slip transfer across α_2 lamellae is thought to be one of the key parameters governing the mechanical strength of the alloy.

The role of the α_2 phase in transmitting slip has been studied by earlier researchers by *post-mortem* transmission electron microscopy conducted on lamellar TiAl-based samples strained at room temperature. Each work has provided different results. Appel *et al*. [3] observed no slip activation in the α_2 lamellae and concluded

*Corresponding author. Email: guy.molenat@cemes.fr
†Reflecting the tetragonal symmetry of TiAl, the $\langle hkl]$ notation allows every permutation between h and k while $\pm l$ is ascribed to the third position [1].

Philosophical Magazine Letters
ISSN 0950-0839 print/ISSN 1362-3036 online © 2006 Taylor & Francis
http://www.tandf.co.uk/journals
DOI: 10.1080/09500830500497066

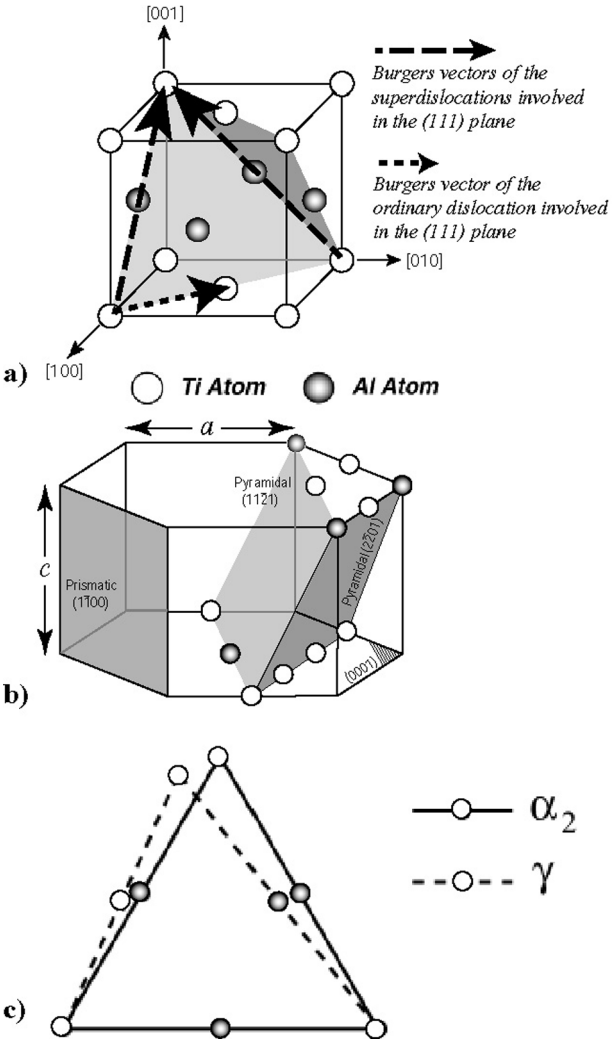

Figure 1. (a) The γ $L1_0$ unit cell. (b) The α_2 $D0_{19}$ structure cell. (c) Schematic representation of the matching of the γ and α_2 structures. Along the close packed directions, the mismatch between the repeat distances in α_2 and γ, along the $\langle 110]$ and $\langle 011]$ directions, is 98.96 and 99.65%, respectively.

that the γ/α_2 interfaces are probably the most effective barriers against twin propagation. On the other hand, Umakoshi *et al.* [4] pointed out prism and pyramidal slip for a loading axis parallel to and perpendicular to the interface, respectively. The micrographs provided in the latter work clearly indicate that these systems are activated on impact of deformation twin on the interface. In more recent studies devoted to the transfer of slip across γ/α_2 interfaces [2, 5, 6] involving twins in the γ phase as the incident system, deformation in α_2 is achieved by **a** dislocations ($\mathbf{b} = 1/3\langle 11\bar{2}0\rangle$) that glide on $\{1\bar{1}00\}$ prism planes. Additional systems such as $1/3\langle 11\bar{2}0\rangle$ on pyramidal $\{2\bar{2}01\}$ [5] or $\{3\bar{3}01\}$ planes [5] and $1/3\langle 11\bar{2}6\rangle$ (dislocations with a **c**-component) on $\{20\bar{2}1\}$ planes [2] and on $\{11\bar{2}1\}$ planes [5] have also

been observed. Godfrey *et al*. [2] concluded that the slip transmission across γ/α_2 interfaces is not common as it requires a high density of dislocations for twins to transfer or for sources to operate. Wiezorek *et al*. [5] also made a similar conclusion on the difficulty of direct slip transmission in α_2 lamellae and suggested stress-induced activation of sources at the interfaces. Lastly, it has been shown that in a fatigued microstructure the $1/3[\bar{2}110](0\bar{1}10)$ glide system can be induced in α_2 lamellae, again as a result of stress concentration at twin spearheads [7].

The present paper is aimed at shedding some light on the conditions by which plasticity is activated within and deformation is transferred through the α_2 lamellae. For this purpose, *in situ* straining experiments have been carried to observe dislocation kinetics under stress in a lamellar Ti–47Al–1Cr–0.2Si alloy at room temperature.

2. Material and experimental method

Arc-melted buttons of Ti–47Al–1Cr–0.2Si (in atomic percentage) were kindly provided by ONERA, Châtillon, France. The as-received buttons were homogenized at 1400°C for 3 h in a platinum furnace under a flowing argon atmosphere and then furnace cooled to room temperature. In this alloy, the average thicknesses of γ and α_2 lamellae are 340 and 115 nm, respectively. Thin slices of about 0.1 mm thickness were cut from the alloy. From these slices, rectangular (1 mm × 3 mm) micro-samples were machined before they were electropolished to produce a thin-edged hole. They were glued on copper grids and observations were made at CEMES (Toulouse, France) in a JEOL 2010 transmission electron microscope operated at 200 kV using a GATAN single-tilt, room-temperature straining device. A detailed description of *in situ* straining experiments has been published elsewhere [8]. We recall that during an *in situ* experiment, a gliding dislocation usually leaves a trace on the two free surfaces of the thin foil as a result of the presence of thin oxides layers. These paired traces allow for an unambiguous, stereographic identification of the slip plane. When necessary, straining was interrupted and the microstructure was recorded under static conditions to complement dislocation analyses.

3. Results

3.1. *Microstructure of the strained area*

Deformation was traced *in situ* in a number of successive lamellae as shown in figure 2. Lamellae L1, L2, L4, L6, L8, L10 and L11 are γ lamellae, whereas the remaining lamellae L3, L5, L7 and L9 are of the α_2 phase. Each γ lamella can assume any one of the six different orientations O1, O2, O3, OT1, OT2 and OT3, such that OT1, OT2 and OT3 are in twin orientation with O1, O2 and O3, respectively. Deformation was studied ahead of a crack tip localized just before lamella L1, which opened progressively during the experiment. As the stress concentration was too high in front of the crack in lamellae L1 and L2, details were hardly visible in TEM: what we could usefully record occurred from lamella L3 onward with further plasticity

Figure 2. Area in which the dynamic sequence represented in figures 3–5 has been recorded with a diffraction vector $\mathbf{g} = \bar{1}11$ and an incident beam direction $\mathbf{B} \approx [16\bar{5}]$. The crack tip is materialized on the left-hand side of the micrograph.

transfer from left to right across subsequent interfaces, up to lamella L11. When the montage shown in figure 2 was taken, deformation driven by stress concentration ahead of the crack tip had already reached the L4/L5 (γ/α_2) interface. Manifestation of localized plasticity that can be seen in the L3 α_2-lamella, consists of a dislocation pile-up in the continuation of the stress concentration generated in lamella L2 by the crack tip. From the location where the pile-up had impacted the L3/L4 (α_2/γ) interface, ordinary screw dislocations with Burgers vector parallel to the interface had originated and spread in the L4 γ-lamella.

3.2. *Dynamic observations*

The deformation response in the L3 α_2-lamella is analysed first for the situation where plasticity is achieved by a dislocation pile-up, moving from left to right and stopping at the next L3/L4 (α_2/γ) interface. Figure 3 shows the corresponding dynamic sequence recorded under weak-beam conditions under the $(20\bar{2}1)_{\alpha 2}$ reflection. The starting configuration is shown in figure 3a. As dislocations are piled-up against the L3/L4 interface, the line joining their upper extremities (see dotted white line in figure 3a) indicates the $(01\bar{1}0)$ prism glide plane. The Burgers vector of the dislocations is $1/3[\bar{2}110]$, the so-called **a**-dislocations, as identified by application of the $\mathbf{g} \bullet \mathbf{b} = 0$ invisibility method (not reproduced here). These slightly bent dislocations make an angle of about 15° to the screw direction. When imaged under weak-beam conditions (figure 3e), they appear to be dissociated into two dislocation partials separated on average by about 11 nm.

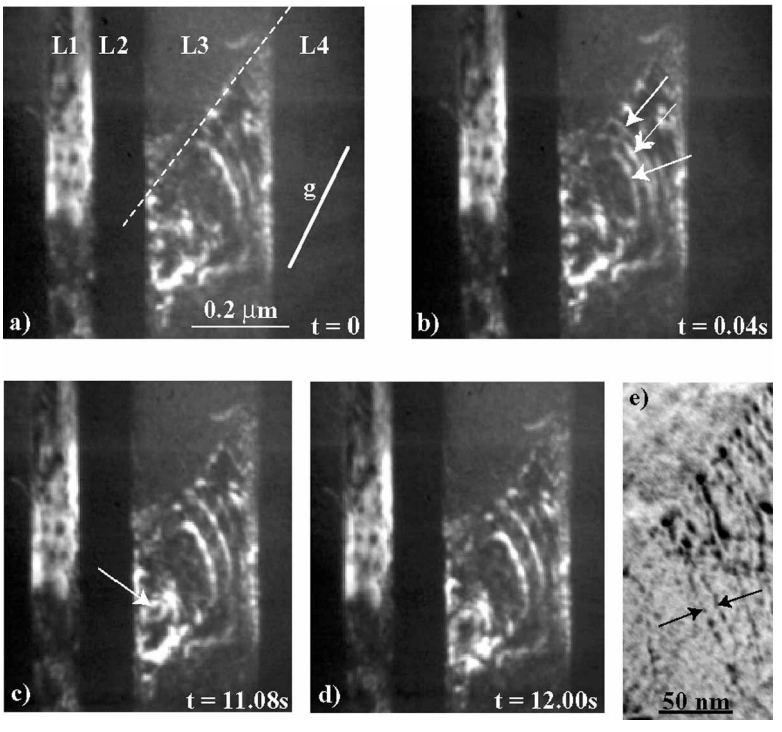

Figure 3. A sequence of snapshots of a dynamic sequence showing the movement of $1/3[\bar{2}110]$ **a**-dislocations in the $(01\bar{1}0)$ prism plane of an α_2 lamella (diffraction vector $\mathbf{g} = 20\bar{2}1$, incident beam direction $\mathbf{B} \approx [\bar{1}2\bar{1}0]$). (a) $t = 0$ s; (b) $t = 0.04$ s; (c) $t = 11.08$ s; (d) $t = 12.0$ s. (e) Evidence for the dissociation of one of the **a**-dislocations under weak-beam conditions (negative print).

Between figure 3a and b, two new dislocations shown by white single-headed arrows (in figure 3b) have incorporated themselves into the pile up. Between figure 3b and c, the dislocation shown by the double-headed arrow in figure 3b has moved away. Incorporation and extraction of individual dislocations in and from the pile-up provide evidence that dislocations are allowed to move individually and therefore that the pile-up is not strictly coplanar. The dislocation loop marked by the arrow in the frame shown in figure 3c was generated within one frame time period in the vicinity of the L2/L3 (α_2/γ) interface. This dislocation remains stable during the next 0.96 s and then opens up at $t = 12.00$ s (figure 3d).

Figure 4 shows a dynamic sequence of bright field images displaying slip transfer across the L3/L4 (α_2/γ) interface under the impact of the above-described $1/3[\bar{2}110](01\bar{1}0)$ pile up. Between $t = 0$ s and $t = 11.12$ s, an **a**-dislocation (arrowed in figure 4b at $t = 0.24$ s) has been added up to the pile-up and a series of slight readjustments have occurred. In less than 0.04 s (two video frames) between $t = 11.12$ s and $t = 11.16$ s, the pile-up moves almost simultaneously toward the L3/L4 interface while some dislocations are emitted in the L4 γ-lamella from the α_2/γ interface. Long arrows in figure 4c ($t = 11.44$ s) indicate two emitted dislocations and the five small arrows underline straight slip traces on one surface reflecting the operation of $(11\bar{1})$ glide. The emitted dislocations are all ordinary screw dislocations with a Burgers vector $(1/2[1\bar{1}0])$ parallel to the interface. It can be noticed that

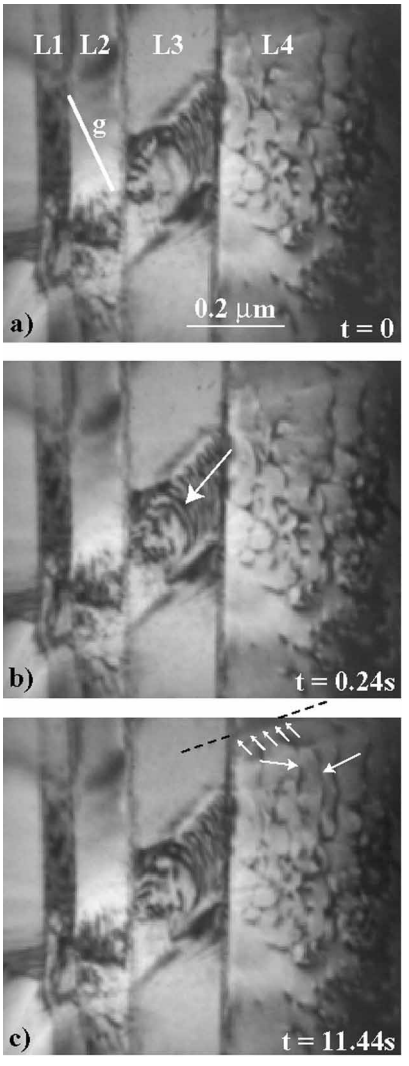

Figure 4. The crossing of an α_2/γ interface (diffraction vector $\mathbf{g}=\bar{1}11$, incident beam direction $\mathbf{B}\approx[16\bar{5}]$). The incident system in L3 lamella is $1/3[\bar{2}110]$ $(01\bar{1}0)$. The emitted dislocations in L4 lamella are $1/2\langle 1\bar{1}0]$ ordinary dislocations. (a) $t=0$ s; (b) $t=0.24$ s; (c) $t=11.44$ s. Slip is significantly more localized in α_2 than in γ. The crack tip is located near the left-hand side bottom corner of the micrographs.

dislocation emission is not strictly limited to the area in contact with the pile-up as exemplified by the slip trace marked in figure 4c.

Whereas figure 4 shows a mode of slip transfer from an α_2 lamella to a γ lamella, Figure 5 displays two reverse situations of a transfer from a γ lamella to an α_2 lamella. In figure 5a and b, the L9 α_2-lamella (left-hand side of the featureless dark slab) is bordered by the L8 and L10 γ-lamellae. Note that under the imaging conditions used in this sequence, L10 together with the L9/L10 interface are not visible. White lines indicate the two interfaces bordering L10. A high density of dislocations and slip traces on the free surfaces can be seen in the L8 as well as in the

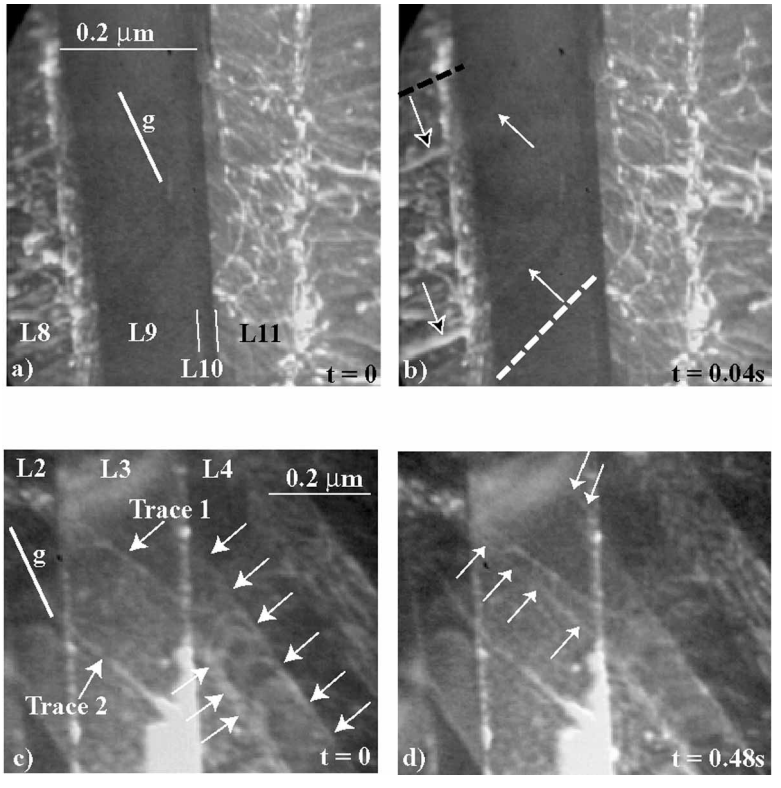

Figure 5. The generation of slip traces illustrating the transfer of γ dislocations into α_2 dislocations. (a) and (b) on the one hand, and (c) and (d) on the other, refer to two distinct areas of the same sample (diffraction vector $\mathbf{g} = \bar{1}11$, incident beam direction $\mathbf{B} \approx [16\bar{5}]$). (a) $t = 0$ s. (b) $t = 0.04$ s showing $[10\bar{1}](\bar{1}11) \rightarrow 1/3[\bar{2}110](01\bar{1}0)$ slip transfer (the slip traces in γ-L8 and in α_2-L9 are indicated by open-headed and white arrows, respectively). (c) $t = 0.2$ s; (d) $t = 0.48$ s. A $1/6[-\bar{1}12]$ $(\bar{1}1\bar{1})$ twin propagating from right to left in γ-L4 generates traces parallel to the $(\bar{2}11\bar{1})$ plane in α_2–L3 (see text).

L11 lamellae. Between figure 5a and b, which are two successive frames, pairs of rectilinear traces appeared in the L8 γ-lamella (the traces indicated by open-headed arrows are parallel to the broken black line) and were prolonged in the L9 α_2-lamella with a change of trace direction (the traces, hardly visible, are indicated by white arrows and are parallel to the broken white line). These traces correspond to $(1\bar{1}1)_{L8}$ and $(01\bar{1}0)_{L9}$ planes, respectively. Their continuity is consistent with a dislocation having crossed through the interface suggesting in turn the transformation of a $[10\bar{1}]$ superdislocation gliding in the $(1\bar{1}1)$ plane into a $1/3[\bar{2}110]$ superdislocation gliding in the $(01\bar{1}0)$ plane (the continuity of both pair of traces means that the intersection of the slip planes lies in the interface, a prerequisite for easy transfer).

The Burgers vectors are parallel to each other and contained in the interface plane. However, since a plenty of 1/2[110] ordinary dislocations, whose Burgers vector is inclined to the interface, are also observed in the L8 γ-lamella, a transfer of these 'inclined' 1/2[110] ordinary dislocations in the γ phase into $1/3[\bar{2}110]$ superdislocations in the α_2 phase cannot be excluded either. In this case, the transfer would be non-direct and would require dislocation reactions relatively more complex with residues left in the interface.

Another situation of a slip transfer from a γ-lamella to an α_2-lamella is presented in figure 5c and d. In this case, the starting configuration (figure 5c) shows a poorly contrasted twin in the L4 γ-lamella (the twin is indicated in figure 5c by two series of white arrows), which had impacted the L4/L3 (γ/α_2) interface from right to left (the movement of the twin is manifested by the curvature of the twinning partials). This motion is opposite to the motion from left to right of dislocations observed in the first stages of deformation. This reversal can be thought of as resulting from the complex stress field induced by the gradual opening of the crack. From the corresponding stereogram, the twin layers on the $(\bar{1}1\bar{1})$ plane and the Shockley dislocations have a $1/6[\bar{1}12]$ Burgers vector. Two traces (labelled Trace 1 and Trace 2), which are not strictly parallel to each other, can be seen in the L3 α_2-lamella. They correspond to the $(\bar{1}100)$ and $(\bar{2}11\bar{1})$ planes, respectively. At $t = 0.40$ s, a new Shockley partial has joined the pile-up pushing the twin towards the L4/L3 interface. Subsequently, a new pair of slip traces (marked by 4 and 2 white arrows in figure 5d) has appeared in L3 in less than 0.08 s. These paired traces are not exactly in the continuity of the traces associated with the twin and they correspond to the $(\bar{2}11\bar{1})$ plane (they are parallel to Trace 2 shown in figure 5c).

For completeness, we have also investigated *post-mortem* deformation microstructures in the same material with particular attention paid to the transfer of deformation across number of α_2 lamellae. Whereas we encountered scarce evidence of dislocations generated in the α_2 phase under the influence of twin impacting the γ/α_2 interface conforming to previously reported observations [2, 5, 6], we have found that α_2 lamellae are quite generally dislocation free. Figure 6 shows the microstructure in a sample compressed at room temperature. In figure 6a,

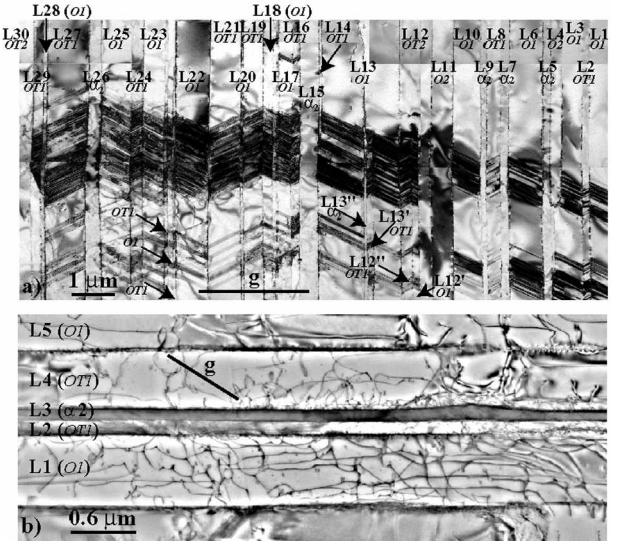

Figure 6. The deformation microstructure in a specimen prepared from a bulk sample compressed at room temperature. (a) An area deformed by twinning (diffraction vector $\mathbf{g} = 111$, incident beam direction $\mathbf{B} \approx [\bar{2}\bar{1}3]$). The decrease from left to right of the average thickness of the twinned region should be noted. The lamellae L12′, L12″, L13′ and L13″ terminate within the observed area. (b) An area deformed by ordinary dislocations (diffraction vector $\mathbf{g} = \bar{1}31$ for the OT1 orientation, incident beam direction $\mathbf{B} \approx [32\bar{3}]$).

the compression axis is parallel to the interface plane. Images produced under different diffracting conditions have all confirmed that the L5, L7, L9, L15 and L26 α_2-lamellae contain no dislocations whereas twinning is observed to have crossed through the whole area massively, probably from left to right as indicated by the decreasing thickness of twinned crystal. Figure 6b displays the same behaviour in an area where deformation in γ lamellae is achieved by ordinary dislocations.

4. Discussion

The present section is aimed at discussing the experimental evidence for slip transfer including how the deformation may propagate throughout the complex lamellar microstructure. It should be kept in mind that because of the proximity of free surfaces in the thin foils used for the *in situ* experiments, a stress concentration is far more rapidly relaxed with distance from the source of stress than in the bulk.

4.1. *Elementary dislocation processes promoting plasticity in the hard phase*

Cutting through α_2 requires (a) the injection of the corresponding dislocations, (b) the propagation of these dislocations in α_2 lamellae and (c) slip transfer at α_2/γ interfaces. These three elementary steps are discussed in the following:

(a) *Injection of dislocations in α_2 lamellae*: two situations have been observed in the present study: (i) the activation of a source in the prism plane within an α_2 lamella (figure 3) and (ii) the transfer of slip from an adjacent γ lamella (figure 5). As to the former situation, it can be inferred from the observation of a closed dislocation loop that the source was located at a distance from the L3/L2 interface (see figure 3c). This implies that the dislocations emitted from the loop in the backward direction (from right to left in figure 3), should be evacuated away from the area where they impacted the L3/L2 interface. That may happen either by annihilation with dislocations incoming from the L2 γ-lamella, or else by cross-slip in basal planes (parallel to the interface). In both cases, this necessary evacuation is assisted by the mismatch stress arising from the semi-coherent matching of the two phases at the interface (figure 1c). The micrographs in figure 5 present two examples of transfer of slip from a γ lamella to an α_2 lamella (situation (ii)). In figure 5a and b, glide planes continuity could be seen and is an evidence of direct slip transfer by a $[10\bar{1}]$ superdislocation of the γ phase into a $1/3[\bar{2}110]$ superdislocation of the α_2 phase. The observation of a transfer in figure 5c and d is similar to events reported in [2, 4–6] since dislocations are emitted in the α_2 lamella under the impact of a twin of the adjacent γ lamella. This slip transfer corresponds to the activation of $1/3[2\ 116]$ $(2\ 111)$ glide, an observation entirely consistent with those of Wiezorek and coworkers [5] who have interpreted it as controlled by the stress-induced activation of an interfacial source.

(b) *Propagation of dislocations in α_2 lamellae*: the glide event observed in the α_2 prism plane is similar to what can be observed in single-phased Ti_3Al alloy [9]. In particular, the dislocation dynamics shown in figure 3, as well as the APB ribbon width determined from figure 3e, indicate that these dislocations are of type II **a**-dislocations (see [9]). **a**-Dislocations can indeed be of two types depending of the

chemical arrangement in the APB plane: type I dislocations induce first-neighbour pairs of aluminium atoms when type II dislocations do not. Type II dislocations are smoothly curved, their dissociation width is about 9 nm and they glide slowly and steadily whereas type I dislocations exhibit rectilinear segments, are more widely dissociated and move in a jerky manner [9]. Type II dislocations represent more than 90% of the mobile dislocations in prismatic planes and are the easiest to activate. On the other hand, the dislocation movements evidenced in figure 5 are swift.

Traces are indeed formed within one video frame (i.e. less than 1/25 s) throughout the entire width of the α_2 phase lamellae (typically 0.2 μm thick). Similarly, the motion of the incoming dislocation (single arrows on figure 3b) or that of the dislocation escaping from the pile-up in the prism plane (double-headed arrow in figure 3b) were also very quick. In fact, the only movements in α_2 that could be traced continuously are those of the dislocations trapped in the pile-up. It should be underlined that *in situ* experiments performed by the Toulouse group under the same experimental procedure have generated dislocation movements slow enough to be observable for the cases of the crossing of γ/γ interfaces in lamellar TiAl alloys [10] and of glide in single-phase α_2 alloys [9]. The differences in dynamics between these and the present observation are significant and thus consistent with the fact that once generated in the α_2 phase, the appropriate dislocations are most certainly submitted to stress levels high enough to enable them to overcome, in less than one twenty-fifth of a second, all the obstacles (frictional forces, extrinsic obstacles) encountered during their flight from one interface to the next. Such a high local stress is attributed to the crack and also to the high density of dislocations in the preceding lamellae. This *in situ* result is consistent with the *post-mortem* observations of Wiezorek *et al.* [11] of the plasticity of α_2-lamellae in specimens fractured at room temperature.

(c) *Slip transfer at α_2/γ interfaces*: Figure 4 shows the transfer of slip across an α_2/γ (L3/L4) interface involving a $1/3\langle 11\bar{2}0\rangle\{1\bar{1}00\}$ system incident in the α_2 phase and a $1/2\langle 1\bar{1}0]\{111\}$ system transferred in the γ phase. There is indeed a continuity of the glide planes of the incident and emitted dislocations. The Burgers vectors of the two types of dislocations (**a**-superdislocations dissociated into paired **a**/2 super-partials and ordinary dislocations) are contained in the interface plane and they are parallel to each other. Each $1/6[\bar{2}110]_{\alpha 2}$ partial dislocation belonging to the $1/3[\bar{2}110]_{\alpha 2}$ superdislocation arriving in the interface plane can thus transform quasi completely into an ordinary dislocation of the γ phase, leaving a residue at the interface. The observation of ordinary dislocations in the γ phase far away from the exact location of the impact (figure 4c) is likely to result from cross-slip in planes parallel to the interface attesting in turn to an overall easiness of slip spreading in the γ phase.

By contrast, the presence of the pile-up in the L3 α_2-lamella reflects that the mechanism involved during slip transfer via dislocations across α_2/γ (L3/L4) interface remains difficult in spite of otherwise favourable crystallographic factors. In practice, the few available examples of a dislocation crossing through α_2 observed in the present work and in the literature [2, 4–7] are all restricted to the simple crystallographic situation that ensures continuity between the glide planes of the incident and emitted dislocations. Furthermore, except for the case of an impact by a twin, the Burgers vector of the incident and emitted dislocations are parallel to each other and are contained into the interface plane.

There is no solid argument that would enable one to decide which of the three (a)–(c) stages of cutting through α_2 is rate controlling. In the α_2 phase, dislocation

mobility is indeed relatively poor, in accordance with the critical resolved shear stresses for deformation in Ti_3Al alloys [12–16] with respect to that of the γ phase [17–19]. The γ/α_2 interface (figure 1c) contains mismatch dislocations which oppose dislocation crossing for both directions of transfer, γ to α_2 or α_2 to γ. Furthermore, for dislocation crossing to take place from γ to α_2, ordinary dislocations must assemble in pairs to produce dislocations that can slip in the α_2 phase, but that is hampered by cross-slip which tends to scatter ordinary dislocations quite significantly (see L4 lamella in figures 2 and 4). Whatever be the rate-controlling step, the difficulty of inducing plasticity in the α_2 phase can be conclusively underlined.

4.2. *The spreading of deformation*

As already mentioned, dislocation activity in α_2-lamellae has been reported from different *post-mortem* observations [2, 4–7, 11] and the present *in situ* experiments have directly evidenced similar situations. Our *post-mortem* investigations performed at a large scale on foils sliced from bulk samples, however, indicate that in most cases the propagation of deformation through α_2-lamellae does not necessitate dislocation activity (figure 6). This not yet analysed feature is not in contradiction with previous *post-mortem* results. The absence of dislocations is usually interpreted under two opposite points of views. One is, of course, that there is no such activity in the material, while the other states that the process is so easy that the corresponding dislocations all disappear leaving less mobile debris throughout the samples. In the present case, because there is no indication of dislocation storage at α_2/γ interfaces, one can safely conclude to the absence of deformation by dislocations throughout the α_2 phase. The question thus arises as to how the spreading of deformation takes place. We propose that this is achieved elastically. The present results clearly indicate that γ/α_2 interfaces are hardly penetrable even under large stress concentration. The elastic deformation of the α_2 phase manifests itself as black lobes of contrast that are currently observed in the vicinity of twin impacts (e.g. in lamella L15 at the L14/L15 interfaces in figure 6a). A similar strain contrast effect had been reported by Wiezorek *et al*. (see figure 2 of [5]). For such an elastic transfer to occur, all that is required is that the twin-induced stress level be sufficient on the other side of the α_2 lamella to activate sources. As the elastic stress decreases within α_2 with increasing distance from the twin tip, the elastically-mediated transfer of deformation is expected to be strongly dependent on thickness of the α_2 lamellae. Consequently, the elastic mediated transfer should cease to occur beyond a certain thickness of the α_2 lamellae. However, in the *post-mortem* study presented in this paper, there is no convincing evidence that twin propagation by elastically mediated transfer was arrested at even thick lamellae (for instance, see L15 in figure 6a). This apparent inconsistency can be explained on the basis of uneven thickness of α_2 lamellae. It is indeed often observed by transmission electron microscopy that γ as well as α_2 lamellae assume a wedge-shape and terminate sometimes in the crystal. Transmission electron microscopic observations give information about lamellar thicknesses within the thin foil but it does not tell whether a given lamella was far thinner or far thicker elsewhere in the grain under investigation. Once nucleated twins propagate not only in transverse direction until the next γ/α_2 interface but also laterally normal to the twin slip plane, as far as the full dimensions of γ lamellae. In the course of their

lateral expansion, the twins thus scan the α_2 lamella that they have to overcome. Since α_2 lamellae are generally not uniformly thick but rather corrugated [20, 21], the twins proceed within a γ-lamella until they encounter a region where the thickness of the obstacle α_2-lamella renders elastically-mediated transfer possible. This is a mechanism by which strain may gradually propagate across a succession of apparently impenetrable α_2 slabs. Forwood and Gibson [6] have suggested a scenario based on twin wrapping around the termination of the α_2 lamella and then invading the next γ slab. Besides clear similarities with the above, the mechanism proposed here corresponds better to the experimental evidence acquired in this investigation, i.e. the frequent observation of twins propagating across tens of lamellae: finding a place where the α_2-lamella thickness could be small enough for an elastic transfer may happen before finding the hypothetic edge of the hard slab for wrapping.

Finally, it is interesting to note that the mechanism achieving strain transfer may differ according to whether deformation is conducted on bulk samples or *in situ* thin foils. To discuss this point, we approximate the twin spearhead to n partial dislocations piled up at equilibrium against some obstacle under the application of a shear stress τ_a. We recall that whether twin impact takes places in the bulk or in a thin foil, the shear stress on the leading dislocation of the pile-up is always $\tau_B = n\tau_a$. Hence, insofar dislocation generation by stress concentration at the twin-impacted γ/α_2 interface is concerned, there should be no significant differences between thin foils and bulk samples. Regarding the alternative process of elastically-mediated activation of dislocation sources in the next γ-lamella, the situation is actually quite different between the bulk samples or thin specimens for two intrinsic reasons. For one, due to the image force, the stress τ_f ahead of a crack, a twin or a pile-up in a thin foil of thickness h decreases exponentially with the distance x from the head of the pile-up [22] roughly as:

$$\tau_f \approx \tau_B \exp[-3x/h].$$

For example, in a foil say 150 nm thick, an α_2 lamella of about 100 nm would then decrease τ_f in the next γ lamella down to 15% of τ_B. It is noticed that the conditions encountered in the *in situ* sequences shown in figures 3 and 4 are already unfavourable since the α_2-lamellae L3 and L9 are about twice as large as the average thickness of α_2-lamellae in the bulk (i.e. approximately 200 nm here for 115 nm in average in the bulk). Hence the stress attenuation seems too large for elastically-mediated transfer to operate in this case. It is thus unlikely that, in the absence of the nearby crack tip, the dislocations would ever have cut through the α_2-lamellae. The second reason hampering elastic transfer originates from geometrical differences between bulk samples and thin specimens. As mentioned earlier, a twin expanding laterally in a given γ lamella of a bulk sample scrutinizes the adjacent α_2 lamella for its weak points along the twin slip plane, thus increasing the probability to encounter one of the few regions where the adjacent α_2 lamella becomes sufficiently thin for deformation to percolate. In other words, the resistance of α_2 slabs to twin propagation is not determined by their mean thickness but, for each lamella, by the thinnest part which is to be impacted by the twin. When propagating in thin foils, it is clear that twins do not have such a degree of freedom, and this is believed to make dislocation generation in α_2-lamellae relatively more likely in thin foils than in bulk samples.

5. Conclusions

The present *in situ* observations of plastically deformed lamellar TiAl have confirmed that, while most of dislocation activity has occurred in the γ phase, dislocation activity has taken place in the α_2 slabs of alloys also. Both *in situ* and *post-mortem* observations indicate that α_2 lamellae seldom happen to yield plastically under the impact of twin spearheads. The deformation modes in the α_2 phase are similar to those observed in the single-phased Ti_3Al alloys. Cutting through a α_2 lamella involves three processes: either the nucleation of dislocations in a given α_2 lamella or the transfer of these from a γ lamella, followed by dislocation glide over the α_2 lamella and the subsequent crossing through α_2/γ interfaces. The three processes are difficult and the rare events of the crossing of γ/α_2 or α_2/γ interfaces that have been observed in the present study correspond to favourable situations in terms of the continuity of Burgers vectors and glide planes. The kinetics of the dislocation glide in the α_2 lamellae is indicative of high local stresses exerted by the crack and by dislocations retained in high densities in the previous γ lamella.

Even if some plasticity is observed in α_2-lamellae in some favourable situations described above, propagation of deformation throughout a lamellar grain across these α_2-slabs should most frequently occur through an elastically-mediated transfer initiated in the thinner parts of the hard lamellae.

Acknowledgements

The authors acknowledge the Indo-French Centre for the Promotion of Advanced Research, New Delhi for sponsoring this project (No. 2308-2) and for funding the visit of one of the authors (JBS) to CEMES Toulouse, France. The authors are also grateful to J. Crestou of CEMES for his help in preparation of the thin foil.

References

[1] G. Hug, A. Loiseau and P. Veyssière, Phil. Mag. A **57** 499 (1988).
[2] A. Godfrey, D. Hu and M.H. Loretto, Phil. Mag. A **77** 287 (1998).
[3] F. Appel, P.A. Beaven and R. Wagner, Acta Metal. Mater. **41** 1721 (1993).
[4] Y. Umakoshi and T. Nakano, Acta Metal. Mater. **41** 1155 (1993).
[5] J.M.K. Wiezorek, X.D. Zhang, W.A.T. Clark, *et al.*, Phil. Mag. A **78** 217 (1998).
[6] C.T. Forwood and M.A. Gibson, Phil. Mag. A **80** 2785 (2000).
[7] T. Nakano, H. Biermann, M. Riemer, *et al.*, Phil. Mag. A **81** 1447 (2001).
[8] A. Couret, J. Crestou, S. Farenc, *et al.*, Microsc. Microanal. Microstruct. **4** 153 (1993).
[9] M. Legros, A. Couret and D. Caillard, Phil. Mag. A **73** 61 (1996).
[10] S. Zghal and A. Couret, Phil. Mag. A **81** 365 (2001).
[11] J.M.K. Wiezorek, P.M. DeLuca, M.J. Mills, *et al.*, Phil. Mag. Lett. **75** 271 (1997).
[12] Y. Umakoshi, T. Nakano, K. Sumino, *et al.*, MRS Symp. Proc. **288** 441 (1993).
[13] Y. Umakoshi, T. Nakano, T. Takenaka, *et al.*, Acta Metal. Mater. **41** 1149 (1993).
[14] H. Inui, Y. Toda, Y. Shirai, *et al.*, Phil. Mag. A **69** 1161 (1994).
[15] Y. Minonishi, M. Otsuka and K. Tanaka, in *Proceedings of the International Symposium on Intermetallics Compounds, Structure and Mechanical Properties*, edited by O. Izumi (Japan Institute of Metals, Sendai, 1999), p. 543.
[16] Y. Minonishi, Phil. Mag. A **63** 1085 (1991).

[17] T. Nakano, K. Matsumoto, T. Seno, *et al*., Phil. Mag. A **74** 251 (1996).
[18] H. Inui, M. Matsumuro, D.H. Wu, *et al*., Phil. Mag. A **75** 395 (1997).
[19] F. Grégori and P. Veyssière, *Gamma Titanium Aluminides*, edited by Y.-W. Kim, D.M. Dimiduk and M.H. Loretto (Minerals, Metals & Materials Society, Warrendale, 1999), pp. 75–82.
[20] S. Zghal, S. Naka and A. Couret, Acta Metall. Mater. **45** (1997).
[21] S. Zghal, M. Thomas, S. Naka, *et al*., Phil. Mag. Lett. **81** 537 (2001).
[22] G. Saada, J. Douin, *et al*., Phil. Mag. **284** 807 (2004).